

Towards Optimal and Scalable Evacuation Planning Using Data-driven Agent Based Models

Kazi Ashik Islam, Da Qi Chen, Madhav Marathe, Henning Mortveit, Samarth Swarup, Anil Vullikanti

Biocomplexity Institute, University of Virginia

{ki5hd,wny7gj,marathe,henning.mortveit,swarup,vsakumar}@virginia.edu

Abstract—Evacuation planning is a crucial part of disaster management where the goal is to relocate people to safety and minimize casualties. Every evacuation plan has two essential components: routing and scheduling. However, joint optimization of these two components with objectives such as minimizing average evacuation time or evacuation completion time, is a computationally hard problem. To approach it, we present MIP-LNS, a scalable optimization method that utilizes heuristic search with mathematical optimization and can optimize a variety of objective functions. We also present the method MIP-LNS-SIM, where we further combine an agent-based model together with MIP-LNS to more accurately estimate the delay on roads due to congestion. We use real-world road network and population data from Harris County in Houston, Texas, and apply our methods to find evacuation routes and schedule for the area. We show that, within a given time limit, MIP-LNS finds better solutions than existing methods in terms of average evacuation time, evacuation completion time and optimality guarantee of the solutions. We also perform experiments with MIP-LNS-SIM to show its efficacy in estimating delays in the road network due to congestion by using an agent based model. Our results show that MIP-LNS-SIM can find efficient evacuation plans, and at the same time provide an estimate of the evacuation completion time for the given plan with a small percent error.

Index Terms—Evacuation, Routing, Scheduling, Agent Based Simulation, NP-hard, Mixed Integer Program, Heuristic, Large Neighborhood Search

I. INTRODUCTION

Evacuation plans are essential to ensure the safety of people living in areas that are prone to potential disasters such as floods, hurricanes, tsunamis and wildfires. Large-scale evacuations have been carried out during the past hurricane seasons in Florida, Texas, Louisiana, and Mississippi. Examples of hurricanes when such evacuations were carried out include, Katrina & Rita (2005), Ike & Gustav (2008), Irma & Harvey (2017), Laura (2020), Ida (2021), and Ian (2022). The most recent category four hurricane, Ian, caused 119 deaths in the state of Florida alone [1]. To give a sense of the scale of evacuations due to such hurricanes, about 2.5 million individuals were evacuated from the coastal areas of Texas [2] before the landfall of Hurricane Rita. At such scale, it is essential to have an evacuation plan to ensure that people can evacuate in a safe and orderly manner. Any such plan needs to have two essential components: (i) Evacuation Routes, which are paths that the evacuees will take to egress out of the area under danger, and (ii) Evacuation Schedule which dictates when people should leave from different regions. The goal

is to find a plan that optimizes a desired objective such as average evacuation time, evacuation completion time.

The focus of our paper is on *jointly optimizing the routes and schedules*. Informally, the idea is to find a time to schedule when individuals can begin evacuation (within a given time window) and a route that would be used to evacuate, so as to minimize the objective functions capturing the system level evacuation time (see Section III for formal definition of the problems). Jointly optimizing over the routes and schedule is significantly harder from a computational standpoint (See Section IV for hardness results). Existing methods, even those designed to find bounded sub-optimal solutions, do not scale to city or county level planning problems. Thus, finding good evacuation routes and schedule within a reasonable amount of time, for a city or county with a large population, remains an open problem. Moreover, during evacuations, large number of people try to egress out of an area in a relatively small amount of time. This results in traffic congestion and huge delays in the evacuation process, presenting another challenge to evacuation planning. It is, therefore, crucial to consider and *model the delays caused by traffic congestion* during the planning phase.

Our Contributions As our **first** contribution, we present MIP-LNS, a scalable optimization method that can find solutions to a class of evacuation planning problems, while optimizing for a variety of objectives. MIP-LNS is designed based on the well known Large Neighborhood Search (LNS) framework. It combines the idea of heuristic search with mathematical optimization (Section III). In this paper, we focus on three objectives: minimizing average evacuation time, minimizing evacuation completion time, and minimizing the average evacuation time of ‘non-outlier’ evacuees (Section III). We show that all of these three optimization problems are hard to approximate within a logarithmic factor (Section IV). In the same section, we also show that even if the underlying graph is a subgraph of a grid, these problems remain NP-hard.

Second, we choose Harris county in Houston, Texas as our study area and apply MIP-LNS. The county has about 1.5 million households and spans an area of 1,778 square miles. We have used real-world road network data from HERE maps [3] and population data generated by Adiga *et al.* [4] to construct a realistic problem instance. The study area has been affected by major hurricanes in the past (e.g. Rita, Ike, Harvey, Laura). Using MIP-LNS, we calculate evacuation routes and schedule. We show that, within a given time limit, MIP-LNS finds solutions that are on average 13%, 20.7% and 58.43%

better than an existing baseline method [5] in terms of average evacuation time, evacuation completion time and optimality guarantee of the solution, respectively (Section VII-B).

Finally, we present MIP-LNS-SIM, where we combine agent-based simulation with MIP-LNS. Specifically, we utilize the agent-based queuing simulation system ‘QueST’ presented by Islam *et al.* [6] to model delays caused by congestion in the road network. We show that by simulating the evacuation of only a portion of the evacuees, we can obtain vital information. Within MIP-LNS-SIM, we iteratively use these simulated results to better predict road congestion in the network. Through our experiments, we show that MIP-LNS-SIM not only finds efficient evacuation plans, but also provides an estimate of evacuation completion time for the plan with a small percent error (Section VII-C).

II. RELATED WORK

Researchers have approached the evacuation planning problem in different ways in the past. Hamacher and Tjandra [7] formulated it as a dynamic network flow optimization problem and introduced the idea of time expanded graphs to solve it using mathematical optimization methods. However, the computational cost of their proposed methodology was prohibitively expensive. This led to several heuristic methods [8]–[10] that are capable of working with larger networks. However, these methods are designed to solve the routing problem only and they either do not consider the scheduling problem at all or propose simple schemes such as letting evacuees leave at a constant rate. On the other hand, in a series of research works, Even and Pillac *et al.* [11], Romanski and Van Hentenryck *et al.* [12], and Hasan and Van Hentenryck [5], [13] considered the joint optimization problem of routing and scheduling. They formulated the problem as Mixed Integer Programs and used decomposition techniques [14], [15] to separate the route selection and scheduling process. A review of existing works on evacuation planning and management can be found in the survey paper by Bayram [16].

The use of convergent evacuation routes has been explored in the literature [5], [11]–[13], where all evacuees coming to an intersection follow the same path afterwards. This is also known as confluent flow [17]. Golin *et al.* [18] investigated the single-sink confluent quickest flow problem where the goal is minimizing the time required to send supplies from sources to a single sink. They showed that the problem cannot be approximated in polynomial time within a logarithm approximation factor. In this paper, we prove that finding evacuation routes and schedule that minimizes average evacuation time is also hard to approximate.

We use the most recent method (Benders Convergent or BC) by Hasan and Van Hentenryck [5] as our baseline and show that MIP-LNS finds better solutions in terms of average evacuation time, evacuation completion time and optimality guarantee of the solution. In addition to the minimizing average evacuation time objective, we provide direct MIP formulations for two other objectives: minimizing the average evacuation time for ‘non-outlier’ evacuees and minimizing the

evacuation completion time. MIP-LNS (as well as MIP-LNS-SIM) is able to optimize all three objectives without needing any modifications.

Heuristic search methods and meta-heuristics are generally applied to problems that are computationally intractable. The goal is to find good solutions in a reasonable amount of time. The Large Neighborhood Search (LNS) framework [19] has been successfully applied to various hard combinatorial optimization problems in the literature [20]. Recently, Li *et al.* [21] applied the LNS framework to find solutions for the Multi-Agent Path Finding Problem where the goal is to find collision free paths for multiple agents.

Agent-based models have been combined with optimization methods in the literature [22]–[25]. For instance, Holmgren and Persson *et al.* [22] combined an agent-based approach with a decomposition based optimization method to solve an integrated production, inventory, and distribution routing problem. In this paper, we have used an agent-based simulator, QueST [6], iteratively to estimate delays in the road network due to congestion. QueST is an agent-based discrete event queuing network simulation system where each edge of the road network is represented as a queue and vehicles are agents that travel through these queues. Given an evacuation plan, in the form of evacuation routes and departure time of evacuees, QueST can simulate an evacuation scenario. We use it to extract information, such as estimated travel time on the roads, and then use it within MIP-LNS-SIM to find efficient evacuation plans.

III. PROBLEM FORMULATION

In this section, we introduce some preliminary terms that we use in our problem formulation. Then we define three different objective functions for the evacuation planning problem. This allows us to formally define the optimization problems A-DCFP, CT-DCFP, and O-DCFP. Next, we describe how we construct time expanded graphs to model the flow of evacuees over time using a sample problem instance. Finally, we present a Mixed Integer Program (MIP) that represents a class of evacuation planning problems and show how we use it to formulate the above mentioned optimization problems.

Definition III.1. A *road network* is a directed graph $\mathcal{G} = (\mathcal{N}, \mathcal{A})$ where every edge $e \in \mathcal{A}$ has (i) a capacity c_e , representing the number of vehicles that can enter the edge at a given time and (ii) a travel time T_e representing the time it takes to traverse the edge.

Definition III.2. Given a road network, a *single dynamic flow* is a flow f along a single path with timestamps a_v , representing the arrival time of the flow at vertex v that obeys the travel times. In other words, $a_v - a_u \geq T_{uv}$. A *valid dynamic flow* is a collection of single dynamic flows where no edge at any point in time exceeds its edge capacity.

Definition III.3. An *evacuation network* is a road network that specifies $\mathcal{E}, \mathcal{S}, \mathcal{T} \subset \mathcal{N}$, representing a set of source, safe and transit nodes respectively. Furthermore, for each source

node $k \in \mathcal{E}$, let $W(k)$ and d_k represent the set of evacuees and the number of evacuees at source k respectively. Let W denote the set of all evacuees.

For the purpose of scheduling an evacuation, we observe that once an evacuee has left their home, it is difficult for them to pause until they reach their desired destination. We also assume that people from the same location evacuate to the same destination. Similarly, we assume that if two evacuation routes meet, they should both be directed to continue to the same location.

Definition III.4. Given an evacuation network, we say a valid dynamic flow is an *evacuation schedule* if the following are satisfied:

- all evacuees end up at some safe node,
- no single dynamic flow has any intermediary wait-time (i.e. $a_v - a_u = T_{uv}$ and,
- the underlying flow (without considering time) is confluent, where if two single dynamic flows use the same vertex (possibly at different times), their underlying path afterwards is identical.

A natural objective to optimize for during evacuation planning is the metric average evacuation time of the evacuees. Optimizing for this objective ensures that the evacuation time of the evacuees, on average, is as small as possible. To define it formally, let t_i denote the evacuation time of evacuee i . We can then formally define the following problem:

Problem 1. Average Dynamic Confluent Flow Problem (ADCFP). Given an evacuation network, let T_{max} represent an upper bound on evacuation time. Find an evacuation schedule such that all evacuees arrive at some safe node before time T_{max} while minimizing $\frac{1}{|W|} \sum_{i \in W} t_i$.

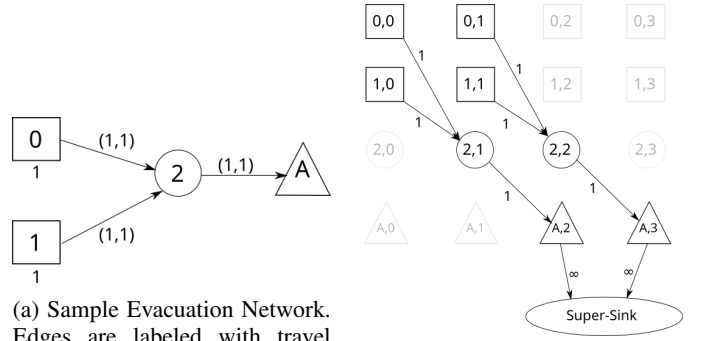
We formally define two other planning problems.

Minimizing Evacuation Completion Time: i.e. time when the last evacuee reaches safety, is another natural objective to optimize during evacuation planning. Formally:

Problem 2. Completion Time Dynamic Confluent Flow Problem (CT-DCFP). Given an evacuation network, find an evacuation schedule such that all evacuees arrive at some safe node while minimizing $\max_{i \in W} t_i$.

Minimizing the Average/Total Evacuation Time of p -fraction of the evacuees: In evacuation scenarios, some evacuees may be in such a situation that the cost of evacuating them may dramatically increase the overall evacuation objective, e.g. the Average Evacuation Time. We consider such evacuees as ‘outliers’. A common way to handle outliers is to optimize the desired objective for the ‘non-outlier’ evacuees, while taking into consideration that the ‘outlier’ evacuees will also evacuate and use the same road network. We formally define the problem as follows:

Problem 3. Outlier Average Dynamic Confluent Flow Problem (O-DCFP). Given an evacuation network, let T_{max} represent an upper bound on evacuation time. Given $p \in [0, 1]$, find



(a) Sample Evacuation Network. Edges are labeled with travel time and flow capacity respectively. Source, safe and transit nodes are denoted by squares, triangles, and circles respectively. Source nodes are labeled with number of evacuees.

(b) Time Expanded Graph (TEG) for the Sample Network. Edges are labeled with capacity. Construction of this TEG sets an upper bound of 3 time units for evacuation completion.

Fig. 1: Sample Problem Instance

an evacuation schedule S such that all evacuees arrive at some safe node before time T_{max} while minimizing $\frac{1}{|W_p|} \sum_{i \in W_p} t_i$ where W_p is the set of p -fraction of the evacuees with the lowest evacuation time in schedule S .

A. Time Expanded Graph for Capturing Flow Over Time

Joint routing and scheduling over networks requires one to study flows over time. However, capturing the flow of evacuees over time using only static flows on the road network is challenging. For instance, let us consider the sample evacuation network shown in Figure 1a. All three edges in this network have a capacity of 1, which means 1 car can enter the link in a single timestep. However, sending flow from both sources (0 and 1) at a rate of 1 evacuee per timestep will not work because then two evacuees will reach node 2 at the same timestep but only one evacuee will be able to enter edge $(2, A)$. The main issue here is that we need to keep track of available capacity on the edges at different points in time. We cannot do it using static flows because static flows have the underlying assumption that flows travel instantaneously. To address this issue, researchers have defined dynamic flows ([26]–[28]) and used time expanded graphs to solve dynamic flow problems ([5], [7], [11], [12]). In this paper, we also use a *time expanded graph (TEG)* to capture the flow of evacuees over time.

Time expanded graph is a directed graph denoted by $\mathcal{G}^x = (\mathcal{N}^x = \mathcal{E}^x \cup \mathcal{T}^x \cup \mathcal{S}^x, \mathcal{A}^x)$. To construct it, we first fix a time horizon \mathcal{H} and discretize the temporal domain into discrete timesteps of equal length. Then we create copies of each node at each timestep within \mathcal{H} . After that, for each edge $e(u, v)$ in the road network, we create edges in the TEG as $e_t(u_t, v_{t+T_e})$ for each $t \leq \mathcal{H} - T_e$ where the edges e_t have the same flow capacity as e . Finally, we add a super sink node v_t that connects to the nodes u_t for each $u \in \mathcal{S}$ and each $t \leq \mathcal{H}$. Edges to the super sink node are assigned an infinite amount of capacity. Note that, when creating the time expanded graph, we are adding an additional dimension (i.e. time) to the road network. *The size of the TEG is about \mathcal{H}*

times as large as the road network in terms of number of nodes and edges. – yielding a substantially larger problem representation. For instance, the original Houston network with about 1330 nodes, a discretization step of 2 minutes and an evacuation horizon of 15 hours yields a time expanded graph with about 600,000 nodes — yielding a 400 times larger TEG. This time expanded representation is one important reason for the underlying computational space and time complexity of the problem and motivates the need for efficient heuristics.

A sample evacuation network and its corresponding TEG with time horizon $\mathcal{H} = 3$ are shown in Figure (1a-1b). The source, safe and transit nodes are denoted by squares, triangles, and circles respectively. In the TEG, there may be some nodes that are (i) not reachable from the source nodes, or (ii) no safe node can be reached from these nodes within the time horizon. These nodes are greyed out in Figure 1b.

An optimal solution of A-DCFP (and CT-DCFP) for this sample problem instance is to use the routes $0 \rightarrow 2 \rightarrow A$ from source node 0 and $1 \rightarrow 2 \rightarrow A$ from source node 1, where the evacuee at source node 0 and 1 leave at timestep 1 and 0 respectively.

B. Mixed Integer Program (MIP) Model

In this section, we present the Mixed Integer Program (1–8) that we use to represent a class of evacuation planning problems. As shown in objective (1), we can have different objectives in the program, each representing a certain planning problem. Here, we use two types of variables: (i) Binary variable $x_e, \forall e \in \mathcal{A}$, which will be equal to one if and only if the edge e is used for evacuation. Otherwise, it will be zero. (ii) Continuous variable $\phi_e, \forall e \in \mathcal{A}^x$, which denotes the flow of evacuees on edge e .

Objective to Optimize (1)

$$s.t. \sum_{e \in \delta^+(k)} x_e = 1 \quad \forall k \in \mathcal{E} \quad (2)$$

$$\sum_{e \in \delta^+(i)} x_e \leq 1 \quad \forall i \in \mathcal{T} \quad (3)$$

$$\sum_{e \in \delta^+(k)} \sum_{t \leq \mathcal{H}} \phi_{e_t} = d_k \quad \forall k \in \mathcal{E} \quad (4)$$

$$\sum_{e \in \delta^-(i)} \phi_e = \sum_{e \in \delta^+(i)} \phi_e \quad \forall i \in \mathcal{N}^x \setminus \{v_t\} \quad (5)$$

$$\phi_{e_t} \leq x_e c_{e_t} \quad \forall e \in \mathcal{A}, t \leq \mathcal{H} \quad (6)$$

$$\phi_e \geq 0 \quad \forall e \in \mathcal{A}^x \quad (7)$$

$$x_e \in \{0, 1\} \quad \forall e \in \mathcal{A} \quad (8)$$

The constraints of the model are explained in Table I. The constraint that evacuation completion time needs to be less than the given upper bound is implicit in the model, as we set the time horizon of the TEG to this upper bound.

To solve A-DCFP using model (1–8), we need to minimize the average evacuation time over all evacuees. To do that, we

	Explanation
Constraint (2)	Ensures that there is only one outgoing edge from each evacuation node.
Constraint (3)	Ensures that at each transit node, there is at most one outgoing edge. This is necessary for convergent routes.
Constraint (4)	Ensures that the total flow coming out of every evacuation node is equal to the number of evacuees at the corresponding node.
Constraint (5)	Flow conservation constraint, incoming flow equals outgoing flow. $\delta^-(i)$ and $\delta^+(i)$ denote the set of incoming and outgoing edges to/from node i , respectively.
Constraint (6)	Flow capacity constraint, flow on an edge will not exceed its capacity. Also, flows are only allowed on assigned edges.
Constraint (7)	Continuous and non-negative flow variables.
Constraint (8)	Binary edge assignment variables.

TABLE I: Model (1–8) Explanation

Underlying Graph	Hardness	Problems		
		A-DCFP	CT-DCFP	O-DCFP
Subgrid/ Planar	NP-hard	Thm. 1	Thm. 1	Thm. 1
General with Two Sources/Sinks	$(3/2 - \epsilon)$ -hard to approx.	Thm. 2	See [18]	Thm. 2
General	$O(\log n)$ -hard to approx.	Thm. 3	See [18]	Thm. 3

TABLE II: Summary of Hardness

first represent the total evacuation time over all evacuees using the variables x_e and ϕ_e as follows:

$$\text{Total Evacuation Time} = \sum_{e \in \delta^-(v_t)} \phi_e t_s(e) \quad (9)$$

Here, $t_s(e)$ denotes the timestep of the starting node of edge e . Dividing (9) by the total number of evacuees will give us the average evacuation time. Note that, minimizing the average evacuation time and the total evacuation time are equivalent as the total number of evacuees is a constant. So, the A-DCFP objective in our MIP model would be: $\min_{x, \phi} \sum_{e \in \delta^-(v_t)} \phi_e t_s(e)$.

Here, we have just provided details on how to formulate A-DCFP as a MIP. Details on how CT-DCFP and O-DCFP are formulated as MIPs are provided in the supplementary materials (Appendix A). Each of the three problems can be solved using our proposed algorithms MIP-LNS and MIP-LNS-SIM.

IV. INAPPROXIMABILITY RESULTS

In this section, we show that the problems we consider are not only NP-hard but also hard to approximate. Even when we consider special planar graphs that perhaps is closer to a city’s road network where G is a subgraph of a grid and all destinations are along the border, these problems remain NP-hard. A summary of the hardness results is found in Table II.

Theorem 1. Problems A-DCFP, CT-DCFP and O-DCFP are NP-hard even if G is a subgraph of a grid and all safety destinations are along the outer boundary.

Theorem 2. For any $\epsilon > 0$, it is NP-hard to approximate A-DCFP and O-DCFP to a factor of $(3/2 - \epsilon)$ of the optimum, even when there are only two sources and one safe node.

Theorem 3. For A-DCFP and O-DCFP with many sources and one safe node, it is NP-hard to approximate within a factor of $O(\log n)$.

To prove Theorem 1, we rely on the general k -Node-Disjoint Path Problem:

Problem 4 (k -Node-Disjoint Path Problem (kNDP)). Given a graph G , a set of k source-sink pairs s_i, t_i , find node-disjoint paths from each source s_i to sink t_i .

The above problem was proven to be hard even when G is a subgraph of a grid [29].

Theorem 4. The k -Node-Disjoint Path Problem is hard to approximate to a factor of $2^{\Omega(\sqrt{\log n})}$ even when the graph is a subgraph of a grid and all sources lie on the outer boundary.

The proofs for Theorem 1, 2, and 3 are provided in the supplementary materials (Appendix E).

V. HEURISTIC OPTIMIZATION

As shown in Section IV, solving A-DCFP, CT-DCFP, and O-DCFP is computationally hard. For this reason, we present the scalable method MIP-LNS where we use MIP solvers in conjunction with heuristic search.

Within MIP-LNS, we first calculate an initial feasible solution in two steps: (i) calculating an initial convergent route set, and (ii) calculating the schedule that minimizes the target objective using the initial routeset. To calculate the initial route set we take a shortest path from each source to its nearest safe node by road. This route set is calculated using Algorithm 3 (Appendix B) to make sure it is convergent. To calculate the schedule, we use the just calculated route set to fix the binary variables x_e in model (1-8). This gives us a linear program that can be solved optimally to get the schedule.

Next, we start searching for better solutions in the neighborhood of the solution at hand (Algorithm 1). Here, we run n iterations. In each iteration, we select $q = (100 - p)\%$ of source locations uniformly at random and keep their routes fixed. This reduces the size of the MIP as we have fixed values for a subset of the variables. We then optimize this ‘reduced’ MIP model using the Gurobi [30] MIP solver. Essentially, we are searching for a better solution in the neighborhood where the selected $q\%$ routes are already decided. Any solution found in the process will also be a feasible solution for the original problem. If we find a better solution with an evacuation completion time T' that is less than the current time horizon (T), then we also update the model by setting the time horizon to T' . When resetting the time horizon, we (i) remove edges in the time expanded graph whose start or end node have a time

Algorithm 1: MIP-LNS Method

Input: Initial solution: sol , Time Expanded Graph: TEG , Time horizon: T , Model to optimize: $model$, (%) of routes to update: p , Number of Iterations: n , Positive number: p_{inc}

Output: Solution of $model$

```

1 for  $l$  to  $n$  do
2   Select  $(100 - p)\%$  of the source locations
   uniformly at random. Let their set be  $S$ .
3   Fix the routes from the source locations in  $S$ . Set
    $x_e = 1$  if  $e$  is on any of the routes from  $S$  in  $sol$ .
4    $sol \leftarrow$  Solution of  $model$  from a MIP solver
5    $T' \leftarrow$  evacuation completion time for solution  $sol$ 
6   if  $T - T' > +threshold$  then
7     Update the  $model$  by setting the time horizon
     to  $T'$ . Prune  $TEG$  and  $model$  by removing:
8     (i) nodes that are unreachable from the
     evacuation nodes within time horizon  $T'$ , and
9     (ii) nodes from which none of the safe nodes
     can be reached within time horizon  $T'$ 
10   $p \leftarrow p + p_{inc}$ 
11 return  $sol$ 

```

stamp greater than T' , and (ii) we prune the TEG by removing nodes that are unreachable from the evacuation nodes, and nodes from which none of the safe nodes can be reached within time T' . This pruning process reduces the number of variables in the MIP model and simplifies the constraints. At the end of each iteration, we increase the value of p by p_{inc} amount. Note that, when $p = 100$, we will be solving the original optimization problem. In our experiments, we set the initial value of p to 75 and used $p_{inc} = 0.5$.

When solving the reduced problem in each iteration (line 4), we use (i) a time limit, and (ii) a parameter $threshold_gap$ to decide when to stop. MIP solvers keep track of an upper bound (Z_U) (provided by the current best solution) and a lower bound (Z_L) (obtained by solving relaxed LP problems) of the objective value. We stop the optimization when the relative gap $(Z_U - Z_L)/Z_U$ becomes smaller than the $threshold_gap$. In our experiments, we set this threshold to 5%. In total, MIP-LNS has four parameters: n , p , p_{inc} , and $threshold_gap$. In some iterations, it may happen that the current solution is already within the threshold gap. In that case, the algorithm will simply continue to the next iteration.

VI. AGENT-BASED MODEL FOR OPTIMIZATION (MIP-LNS-SIM)

In our formulation (Section III), we assume the travel time on each edge to be a constant. This means, as long as there is capacity available on an edge e , vehicles can enter e and they will traverse e in a constant amount of time. A naive estimate of this travel time can be, the time it takes to traverse the edge at speed limit. However, in practice, travel time on a road is affected by the number of vehicles on it. Moreover, travel time on an edge also affects how many cars can enter it

in a given amount of time (i.e. flow capacity of the edge) [31, Chapter 5]. For instance, a higher travel time implies lower speed which then implies lower flow capacity.

Existing research works have used traffic models to predict travel time on edges based on the number of vehicles [31], [32]. To estimate a realistic travel time on the edges during evacuation, we use the agent-based queuing network simulation system Quest with the logistic traffic model [6]. Within the QueST simulator, roads are represented by queues and evacuees are agents that traverse these queues. Given the evacuation routes and schedule (i.e. departure time of evacuees from their initial location), we can simulate the evacuation process using QueST and determine the average travel time on each edge during evacuation. This provides us a reasonable estimate of travel time on the edges when certain routes and schedule are used. However, simulating the evacuation of the entire population is a time consuming task. Therefore, we only simulate the evacuation of a certain percentage of the evacuees at each source and then calculate the average travel time on the edges. Our intuition for this is, the general congestion situation (on roads) during an actual evacuation can be estimated by simulating the evacuation of a portion of the evacuees.

Algorithm 2: MIP-LNS-SIM Method

Input: Evacuation network: \mathcal{G} , Initial solution: sol ,
Time horizon: T , Number of iterations: m ,
Percentage of Evacuees to simulate: p_e

Output: Evacuation routes and schedule.

```

1 for each edge  $e \in \mathcal{A}$  do
2    $T_e \leftarrow$  Time it takes to traverse  $e$  at speed limit on
    $e$ .
3    $c_e \leftarrow$  Updated flow capacity of  $e$ .
4 for 1 to  $m$  do
5    $TEG \leftarrow$  Time expanded graph of  $\mathcal{G}$  with time
   horizon  $T$ , and current travel time, capacity
   values of the edges.
6    $model \leftarrow$  MIP model (1–8) from  $\mathcal{G}$  and  $TEG$ .
7    $sol \leftarrow$  Solution of  $model$  from MIP-LNS.
8   Simulate evacuation of  $p_e\%$  evacuees at each
   source using QueST with routes and schedule
   from  $sol$ .
9   for each edge  $e \in \mathcal{A}$  do
10     $T_e \leftarrow$  Average travel time on  $e$  in simulation
    result.
11     $c_e \leftarrow$  Updated flow capacity of  $e$ .
12 return  $sol$ 

```

Based on the above idea, we present the method MIP-LNS-SIM (Algorithm 2). Here, we first assume that vehicles travel on each edge at the maximum speed allowed and calculate the travel time and flow capacity accordingly (line 1–3). We then create the time expanded graph based on these values and construct the MIP. Next, We solve the MIP model using MIP-LNS. We use the routes and schedule given by the solution to simulate the evacuation of $p_e\%$ of the evacuees at each source.

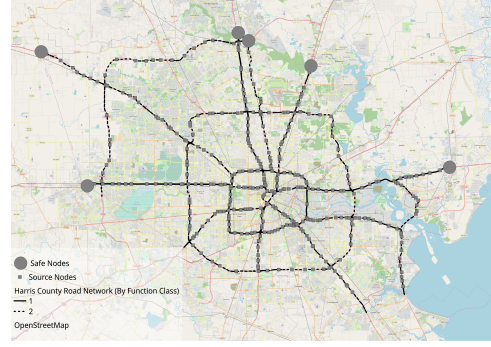


Fig. 2: Harris County Problem Instance

From the simulation results, we calculate the average travel time on each edge and update the travel time as well as the flow capacity of the edges (Details of calculation in Appendix D). We do this iteratively for m times. In our experiments, we have tested with $p_e = 5, 10$ and $m = 10$.

VII. EXPERIMENTS

In this section, we first present details of our problem instance (Section VII-A). Then, we present our experiment results with MIP-LNS and compare the solutions found with the baseline method (Section VII-B). Section (VII-C) contains our experiment results with MIP-LNS-SIM demonstrating how we use the QueST simulator effectively in our optimization process.

A. Problem Instance

In our experiments, we used Harris County in Houston, Texas as our study area. It is situated on the Gulf of Mexico and is prone to hurricanes every year during hurricane season. We have used data from HERE maps [3] to construct the road network. The network contains roads of five (1 to 5) different function classes, which correspond to different types of roads. For instance, function class 1 roads are the major highways or freeways, and function class 5 roads are roads in residential areas. The road network has a hierarchical structure where lower-level roads (e.g., function class 3/4) and the higher-level roads (e.g., function class 1/2) are connected through entrance and exit ramps.

For the purposes of our experiments, we consider the nodes (of the road network) which connect and lead from function class 3/4 roads to function class 1/2 roads as the start/source locations of the evacuees (i.e., the evacuation nodes). We then consider the problem of (i) when should evacuees target to enter the function class 1/2 roads and (ii) how to route them through the function class 1/2 roads to safety. As safe locations, we selected six locations at the periphery of Harris County which are on major roads. A visualization of the dataset is presented in Figure 2. Additional details regarding the road network, the study area, the time expanded graph and the corresponding MIP model are provided in Table III.

We use a synthetic population (as described by Adiga *et al.* [4]) to determine the location of the households. We

# of nodes, edges in the road network	1338, 1751
# of (evacuee) source locations	374
# of Households in the study area	~ 1.5M
Time Horizon	15 Hours
Length of one time unit	2 minutes
# of nodes, edges in the TEG	684.7K, 841.6K
# of binary, continuous variables in A-DCFP MIP	1751, 843.7K
# of Constraints in A-DCFP MIP	1.4M

TABLE III: Problem Instance Details

consider that one vehicle is used per household for evacuation. From this data, we first extract the location of each household. Then, we assign the nearest exit ramp to each household as their source location.

B. MIP-LNS Results and Comparison with Baseline

We performed all our experiments and subsequent analyses on a high-performance computing cluster, with 128GB RAM and 4 CPU cores allocated to our tasks. In addition to MIP-LNS, we used two more methods to solve A-DCFP. We used a time limit of one hour for each method and compared the best solutions found within this time. The three methods we experimented with are:

- 1) Gurobi MIP solver to solve A-DCFP directly.
- 2) Benders Convergent (BC) method, designed by Hasan and Van Hentenryck [5]. We repurposed this method to solve A-DCFP. To the best of our knowledge, there is no publicly available implementation of the method (or the dataset used by the authors). We, therefore, implemented it and plan to make it public.
- 3) MIP-LNS.

1) *Gurobi*: In this experiment, we used Gurobi [30] to directly solve model (1-8) with the A-DCFP objective, for our problem instance. Gurobi was not able to find any feasible solution within the one hour time limit. However, Gurobi was able to come up with a lower bound for the objective value.

2) *Benders Decomposition*: Hasan and Hentenryck [5] presented Benders Convergent (BC) method to solve the ‘Convergent Evacuation Planning’ problem. Their problem is similar to A-DCFP, differing in the objective function, which is maximizing flow of evacuees instead of minimizing average evacuation time. We repurposed their method to solve A-DCFP and used it as our baseline. At the end of the one hour time limit, we got a solution with average evacuation time of 2.54 hours and evacuation completion time of 7.83 hours.

An advantage of using BC method is that, in addition to finding solutions to a problem, it can provide lower bounds for the objective value. However, when we used it for our problem instance of A-DCFP, the method was not able to come up with a lower bound better than the trivial value of zero, due to the size of the problem instance. We, therefore, used the lower

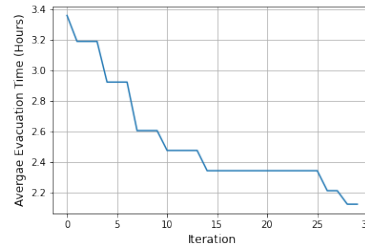


Fig. 3: Average evacuation time over iterations. The decrease in average evacuation time indicates improvement of the objective over the iterations.

bound found by Gurobi to calculate the optimality guarantee of the solution. The optimality guarantee was $\sim 20.47\%$.

3) *MIP-LNS*: In our experiments with MIP-LNS, for A-DCFP, we used thirty iterations with a total time limit of one hour (same as the baseline). Also, since we have a random selection process within MIP-LNS, we ran ten experiment runs with different seeds. To compare the quality of our solutions with the baseline, we use three metrics: average evacuation time, evacuation completion time, and optimality guarantee. Optimality guarantee is defined as follows: let the objective value of the solution sol be z_{sol} and the optimal objective be z_{opt} . Then, the optimality guarantee of sol is $(z_{sol} - z_{opt}) / z_{sol}$, i.e. the smaller the value of optimality guarantee, the better. Table IV shows a comparison of our solutions with the baseline ones in terms of the three metrics. We observe that even the worst solution from MIP-LNS, over the ten experiment runs, is better than the baseline in terms of all three metrics. The best and the average result from MIP-LNS, therefore, also outperform the baseline.

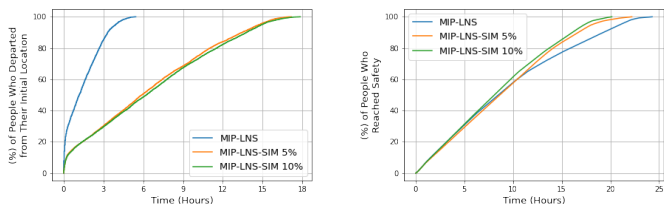
Let the value of a metric m for the baseline and the MIP-LNS solution be m_{base} and m_{lns} respectively. Then, we quantify the improvement over the baseline as $(m_{base} - m_{lns}) / m_{base}$. On average, we see an improvement of 13%, 21%, and 58% over the baseline in the three above-mentioned metrics respectively. This indicates that MIP-LNS finds better solutions than the baseline within the given time limit.

To visualize the progress of MIP-LNS over the iterations, we look at the experiment run that returned the best solution. Figure 3 shows the average evacuation time of the evacuees at different iterations of MIP-LNS. At iteration zero, we have our initial solution that has an average evacuation time of 3.36 hours and an evacuation completion time of 13.5 hours. After thirty iterations, MIP-LNS returned a solution with an average evacuation time of 2.12 hours and an evacuation completion time of 5.77 hours.

We also applied MIP-LNS to find solutions of CT-DCFP and O-DCFP for our problem instance. Due to limited space, we provide the results in Appendix C. In general, the experiment results show that MIP-LNS and our formulation can effectively solve evacuation planning problems with different objectives.

Metric	Baseline [5]	MIP-LNS				Average Improvement
		Best	Worst	Average	Std. Dev.	Over Baseline (%)
Average evacuation time (hours)	2.54	2.12	2.32	2.21	0.06	13
Evacuation completion time (hours)	7.83	5.77	6.83	6.21	0.35	20.69
Optimality guarantee (%)	20.47	4.92	13	8.51	2.43	58.43

TABLE IV: MIP-LNS results for A-DCFP over ten experiment runs and comparison with the baseline method [5] in terms of three metrics: average evacuation time, evacuation completion time and optimality guarantee. Even the worst solution from MIP-LNS outperforms the baseline in terms of all three metrics. On average, we see a $\sim 13\%$, $\sim 21\%$, and $\sim 58\%$ improvement in the three metrics respectively.



(a) Departure rate of evacuees. We observe that in the MIP-LNS solution, evacuees leave very early compared to the solutions from MIP-LNS-SIM-5% and MIP-LNS-SIM-10%.

(b) Arrival rate of evacuees at safe locations. MIP-LNS-SIM-10% has the best evacuation rate and evacuation completion time, followed by MIP-LNS-SIM-5% and then MIP-LNS.

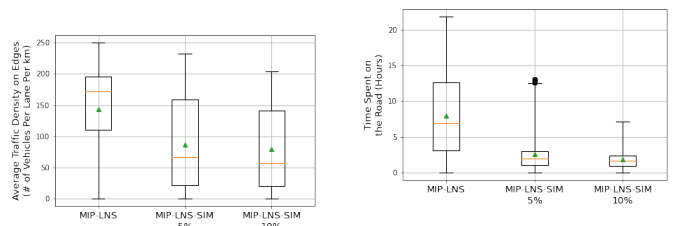
Fig. 4: Comparison of MIP-LNS, MIP-LNS-SIM-5%, and MIP-LNS-SIM-10% in terms of departure rate from sources and arrival rate at safe nodes. Even though MIP-LNS-SIM-5%, and MIP-LNS-SIM-10% regulates the departure of evacuees, they evacuate everyone faster than MIP-LNS.

C. MIP-LNS-SIM Results

So far in our experiments, we assumed that vehicles travel on edges at the maximum speed allowed (on those edges) and calculated the travel time and flow capacity of the edges accordingly. In this section, we present our experiment results with MIP-LNS-SIM where we use the QueST simulator to estimate these values.

Within MIP-LNS-SIM, we set the parameter $m = 10$. We then experimented with two values for the parameter p_e , which are 5, 10. We refer to these two settings as MIP-LNS-SIM-5% and MIP-LNS-SIM-10%. We ran MIP-LNS-SIM with the two settings and found two different solutions. We then performed agent-based simulations of the entire evacuation process (i.e. evacuate 100% of the evacuees) using a solution of MIP-LNS and then also using solutions from MIP-LNS-SIM-5% and MIP-LNS-SIM-10%. We again used the QueST simulator with the logistic traffic model here. We now compare the simulation results.

Figure (4a) shows the departure rate of the evacuees from their initial locations, in the final solution of MIP-LNS, MIP-LNS-SIM-5%, and MIP-LNS-SIM-10%. We observe that, MIP-LNS-SIM-5%, and MIP-LNS-SIM-10% regulates the departure of evacuees to a significant extent (compared to MIP-LNS). As evacuees leave late in these solutions, we might expect the evacuation completion time to be higher



(a) Boxplots showing average traffic density (NO. of vehicles per lane per km) on edges over the evacuation time period. Average traffic density is considerably low in the MIP-LNS-SIM-5% and MIP-LNS-SIM-10% solutions compared to MIP-LNS.

(b) Boxplots showing time spent on the road by evacuees. Due to congestion (as in seen Figure 5a), evacuees spend a significantly larger amount of time on the road in the MIP-LNS solution, compared to MIP-LNS-SIM-5%, MIP-LNS-SIM-10% solutions.

Fig. 5: Congestion on the roads in terms of traffic density and time spent on the road by evacuees.

in these solutions compared to MIP-LNS. Surprisingly, we observe in Figure (4b) that the evacuation completion time is actually smaller in MIP-LNS-SIM-5%, and MIP-LNS-SIM-10% compared to MIP-LNS. This implies that although evacuees left early in the MIP-LNS solution, they could not reach safety early due to the resulting congestion on the roads. In the MIP-LNS-SIM-5% and MIP-LNS-SIM-10% solutions, evacuees departed from their initial location over a longer period of time. This way there was less congestion on the road and the evacuation was completed early even though many people started late.

Figure (5a–5b) verifies our last statement. We see that traffic density on edges, which is the number vehicles per lane and per km, is higher in the MIP-LNS solution (than MIP-LNS-SIM-5%, MIP-LNS-SIM-10%) throughout the evacuation time period. The higher traffic density then causes the evacuees to spend more time on the road. All of these results indicate that MIP-LNS-SIM is better at planning the evacuation than MIP-LNS in terms of reducing congestion on the road during evacuation. This shows the usefulness of an agent-based simulator in evacuation planning.

Finally, Table V shows the estimated and the simulated evacuation completion time for MIP-LNS, MIP-LNS-SIM-5%, and MIP-LNS-SIM-10%. For instance, MIP-LNS predicts that when using the routes and schedule provided by its solution, the evacuation will be completed within 5.77 hours.

Algorithm	Estimated ECT (Hours)	Simulated ECT (Hours)	(%) Error
MIP-LNS	5.77	24.29	76.25
MIP-LNS-SIM-5%	18.43	22.2	16.98
MIP-LNS-SIM-10%	18.97	20.15	5.86

TABLE V: Estimated and simulated Evacuation Completion Time(ECT) for MIP-LNS, MIP-LNS-SIM-5%, and MIP-LNS-SIM-10%. We observe that the percent error of the estimated value decreases significantly with $p_e = 5$ and 10. However, when simulated, it actually took 24.29 hours to evacuate everyone. We observe in Table V that the percent error in estimation decreases considerably in MIP-LNS-SIM-5% and MIP-LNS-SIM-10% where we have used $p_e = 5$ and 10 respectively. The lower percent error is earned at a cost of higher algorithm run time (MIP-LNS-SIM-5%: ~ 6.5 hours, and MIP-LNS-SIM-10%: ~ 7.55 hours).

VIII. CONCLUSION

In this paper, we have presented a general-purpose optimization method MIP-LNS to solve a class of evacuation planning problems. We demonstrated its efficacy by applying it on our study area of Harris county, Houston, Texas. We showed that, for our problem instance, MIP-LNS finds solutions that are on average 13%, 21% and 58% better than the baseline method in terms of average evacuation time, evacuation completion time and optimality guarantee of the solution respectively. We also utilized the agent-based simulator QueST to estimate delays in the road network due to congestion and combined it with MIP-LNS to design the method MIP-LNS-SIM. Through our experiments, we showed that MIP-LNS-SIM can find efficient evacuation plans and provide estimated evacuation completion time for the plans with small percent error.

REFERENCES

- [1] F. D. of Law Enforcement, "Update: Florida medical examiners commission hurricane ian deaths," Oct 2022, [Online]; Accessed 28 Oct 2022. [Online]. Available: [https://www.fdle.state.fl.us/News/2022/October/Update-Florida-Medical-Examiners-Commission-H-\(15\)](https://www.fdle.state.fl.us/News/2022/October/Update-Florida-Medical-Examiners-Commission-H-(15))
- [2] S. K. Carpender, P. H. Campbell, B. J. Quiram, J. Frances, and J. J. Artzberger, "Urban evacuations and rural america: lessons learned from hurricane rita," *Public Health Reports*, vol. 121, no. 6, pp. 775–779, 2006.
- [3] "HERE Premium Streets Data set for the U.S." 2020. [Online]. Available: <https://www.here.com/>
- [4] A. Adiga, A. Agashe, S. Arifuzzaman, C. L. Barrett, R. J. Beckman, K. R. Bisset, J. Chen, Y. Chungback, S. G. Eubank, S. Gupta, M. Khan, C. J. Kuhlman, E. Lofgren, B. L. Lewis, A. Marathe, M. V. Marathe, H. S. Mortveit, E. Nordberg, C. Rivers, P. Stretz, S. Swarup, A. Wilson, and D. Xie, "Generating a synthetic population of the United States," *Network Dynamics and Simulation Science Laboratory*, Tech. Rep. NDSSL 15-009, 2015. [Online]. Available: <https://nssac.bii.virginia.edu/~swarup/papers/US-pop-generation.pdf>
- [5] M. Hafiz Hasan and P. Van Hentenryck, "Large-scale zone-based evacuation planning—part i: Models and algorithms," *Networks*, vol. 77, no. 1, pp. 127–145, 2021.
- [6] K. A. Islam, M. Marathe, H. Mortveit, S. Swarup, and A. Vullikanti, "A simulation-based approach for large-scale evacuation planning," in *2020 IEEE International Conference on Big Data (Big Data)*. IEEE, Dec. 2020. [Online]. Available: <https://doi.org/10.1109/bigdata50022.2020.9377794>
- [7] H. Hamacher and S. Tjandra, "Mathematical modeling of evacuation problems: A state of the art," *Pedestrian and Evacuation Dynamics*, vol. 2002, 01 2002.
- [8] Q. Lu, B. George, and S. Shekhar, "Capacity constrained routing algorithms for evacuation planning: A summary of results," in *Proceedings of the 9th International Conference on Advances in Spatial and Temporal Databases*, ser. SSTD'05. Berlin, Heidelberg: Springer-Verlag, 2005, pp. 291–307. [Online]. Available: http://dx.doi.org/10.1007/11535331_17
- [9] S. Kim, B. George, and S. Shekhar, "Evacuation route planning: Scalable heuristics," in *Proceedings of the 15th Annual ACM International Symposium on Advances in Geographic Information Systems*, ser. GIS '07. New York, NY, USA: ACM, 2007, pp. 20:1–20:8. [Online]. Available: <http://doi.acm.org/10.1145/1341012.1341039>
- [10] K. Shahabi and J. P. Wilson, "CASPER: Intelligent capacity-aware evacuation routing," *Computers, Environment and Urban Systems*, vol. 46, pp. 12–24, Jul. 2014. [Online]. Available: <https://doi.org/10.1016/j.compenvurbsys.2014.03.004>
- [11] C. Even, V. Pillac, and P. Van Hentenryck, "Convergent plans for large-scale evacuations," in *Proceedings of the AAAI Conference on Artificial Intelligence*, vol. 29, no. 1, 2015.
- [12] J. Romanski and P. Van Hentenryck, "Benders decomposition for large-scale prescriptive evacuations," in *Thirtieth AAAI Conference on Artificial Intelligence*, 2016.
- [13] M. H. Hasan and P. Van Hentenryck, "Large-scale zone-based evacuation planning, part ii: Macroscopic and microscopic evaluations," *Networks*, vol. 77, no. 2, pp. 341–358, 2021.
- [14] J. F. Benders, "Partitioning procedures for solving mixed-variables programming problems," *Numerische mathematik*, vol. 4, no. 1, pp. 238–252, 1962.
- [15] T. L. Magnanti and R. T. Wong, "Accelerating benders decomposition: Algorithmic enhancement and model selection criteria," *Operations Research*, vol. 29, no. 3, pp. 464–484, Jun. 1981. [Online]. Available: <https://doi.org/10.1287/opre.29.3.464>
- [16] V. Bayram, "Optimization models for large scale network evacuation planning and management: A literature review," *Surveys in Operations Research and Management Science*, vol. 21, no. 2, pp. 63–84, Dec. 2016. [Online]. Available: <https://doi.org/10.1016/j.sorms.2016.11.001>
- [17] J. Chen, R. Rajaraman, and R. Sundaram, "Meet and merge: Approximation algorithms for confluent flows," *Journal of Computer and System Sciences*, vol. 72, no. 3, pp. 468–489, May 2006. [Online]. Available: <https://doi.org/10.1016/j.jcss.2005.09.009>
- [18] M. J. Golin, H. Khodabande, and B. Qin, "Non-approximability and polylogarithmic approximations of the single-sink unsplittable and confluent dynamic flow problems," in *ISAAC*, 2017.
- [19] P. Shaw, "Using constraint programming and local search methods to solve vehicle routing problems," in *Principles and Practice of Constraint Programming — CP98*. Springer Berlin Heidelberg, 1998, pp. 417–431. [Online]. Available: https://doi.org/10.1007/3-540-49481-2_30
- [20] D. Pisinger and S. Ropke, "Large neighborhood search," in *Handbook of Metaheuristics*. Springer International Publishing, Sep. 2018, pp. 99–127. [Online]. Available: https://doi.org/10.1007/978-3-319-91086-4_4
- [21] J. Li, Z. Chen, D. Harabor, P. J. Stuckey, and S. Koenig, "Anytime multi-agent path finding via large neighborhood search," in *Proceedings of the Thirtieth International Joint Conference on Artificial Intelligence*. International Joint Conferences on Artificial Intelligence Organization, Aug. 2021. [Online]. Available: <https://doi.org/10.24963/ijcai.2021/568>
- [22] J. Holmgren, J. A. Persson, and P. Davidsson, "Agent based decomposition of optimization problems," in *First International Workshop on Optimization in Multi-Agent Systems*, 2008.
- [23] —, "Agent-based dantzig-wolfe decomposition," in *KES International Symposium on Agent and Multi-Agent Systems: Technologies and Applications*. Springer, 2009, pp. 754–763.
- [24] —, "Improving multi-actor production, inventory and transportation planning through agent-based optimization," in *Agent and Multi-Agent Systems in Distributed Systems-Digital Economy and E-Commerce*. Springer, 2013, pp. 1–31.
- [25] P. Davidsson, "Intelligent transport and energy systems using agent technology," in *SCAI*, 2013, pp. 3–10.
- [26] R. K. Ahuja, T. L. Magnanti, and J. B. Orlin, "Network flows," 1988.
- [27] L. R. Ford and D. R. Fulkerson, "Flows in networks," in *Flows in Networks*. Princeton university press, 2015.
- [28] M. Skutella, "An introduction to network flows over time," in *Research trends in combinatorial optimization*. Springer, 2009, pp. 451–482.
- [29] J. Chuzhoy, D. H. Kim, and R. Nimavat, "New hardness results for routing on disjoint paths," in *Proceedings of the 49th Annual ACM SIGACT Symposium on Theory of Computing*, 2017, pp. 86–99.

- [30] Gurobi Optimization, LLC, “Gurobi Optimizer Reference Manual,” 2021. [Online]. Available: <https://www.gurobi.com>
- [31] F. L. Mannering and S. S. Washburn, *Principles of highway engineering and traffic analysis*. John Wiley & Sons, 2020.
- [32] H. Wang, J. Li, Q.-Y. Chen, and D. Ni, “Logistic modeling of the equilibrium speed–density relationship,” *Transportation research part A: policy and practice*, vol. 45, no. 6, pp. 554–566, 2011.
- [33] V. Guruswami, S. Khanna, R. Rajaraman, B. Shepherd, and M. Yannakakis, “Near-optimal hardness results and approximation algorithms for edge-disjoint paths and related problems,” *Journal of Computer and System Sciences*, vol. 67, no. 3, pp. 473–496, 2003.
- [34] S. Fortune, J. Hopcroft, and J. Wyllie, “The directed subgraph homeomorphism problem,” *Theoretical Computer Science*, vol. 10, no. 2, pp. 111–121, 1980.
- [35] G. Naves, N. Sonnerat, and A. Vetta, “Maximum flows on disjoint paths,” in *Approximation, Randomization, and Combinatorial Optimization. Algorithms and Techniques*. Springer, 2010, pp. 326–337.
- [36] N. Robertson and P. D. Seymour, “Graph minors. xiii. the disjoint paths problem,” *Journal of combinatorial theory, Series B*, vol. 63, no. 1, pp. 65–110, 1995.
- [37] A. Adiga, M. Marathe, H. Mortveit, S. Wu, and S. Swarup, “Modeling urban transportation in the aftermath of a nuclear disaster: The role of human behavioral responses,” in *The Conference on Agent-Based Modeling in Transportation Planning and Operations*, Blacksburg, VA, Sep 30 - Oct 2 2013.

APPENDIX A

FORMULATING CT-DCFP AND O-DCFP AS MIXED INTEGER PROGRAMS

In this section, we present the details of how we formulate CT-DCFP and O-DCFP as MIPs. Note that, both of these problems can be solved using MIP-LNS without making any changes to the algorithm.

A. CT-DCFP

Evacuation completion time cannot be represented as a linear function of the variables x, ϕ . To optimize for this objective we modify the time expanded graph as follows: we add a new node z_t for each timestep $t \leq \mathcal{H}$. Then, we add an edge from each safe node $(node, t) \in \mathcal{S}^x$ to the node z_t . Finally, we add an edge from node $z_t, \forall t \leq \mathcal{H}$ to the super-sink (v_t) . Figure 6 shows an example with two safe nodes on how to do this construction.

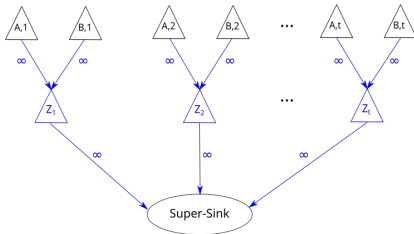


Fig. 6: Modification of the time expanded graph for minimizing evacuation completion time. In this example, we have two safe nodes A and B. Blue nodes and edges are newly added to the TEG. Edges are labeled with their capacity.

With the new time expanded graph, we can represent the evacuation completion time (ECT) as follows:

$$ECT = \max_{e \in \delta^-(v_t)} \mathbb{1}[\phi_e > 0] t_s(e) \quad (10)$$

Here, $t_s(e)$ denotes the timestep of the starting node of edge e . $\mathbb{1}$ denotes the indicator function, i.e.

$$\mathbb{1}[\phi_e > 0] = \begin{cases} 1 & \text{if } \phi_e > 0 \\ 0 & \text{otherwise} \end{cases}$$

As (10) contains the indicator function, we introduce binary variables $y_e, \forall e \in \delta^-(v_t)$ and enforce that: $\phi_e > 0 \iff y_e = 1$. We can do it by adding the following constraints to model (1–8):

$$\phi_e \geq \epsilon - M(1 - y_e) \quad \forall e \in \delta^-(v_t) \quad (11)$$

$$\phi_e \leq M y_e \quad \forall e \in \delta^-(v_t) \quad (12)$$

Here, ϵ is a small positive constant (e.g. 0.001) and M is a positive constant which is equal to the total number of evacuees. With these new variables and constraints, we can now represent ECT as:

$$ECT = \max_{e \in \delta^-(v_t)} y_e t_s(e) \quad (13)$$

By minimizing (13) with model (2–8,11–12) we can achieve the goal of minimizing evacuation completion time.

B. O-DCFP

To optimize the objective of O-DCFP, we extend the time expanded graph (TEG) as follows: First, we add a new ‘bypass’ node $(A', 0)$ to the TEG. Then, from each safe node $s \in \mathcal{S}^x$, we add an edge to $(A', 0)$ with infinite capacity. Finally, we add an edge from $(A', 0)$ to the super-sink (v_t) with capacity $(\sum_{k \in \mathcal{E}} d_k) * (100 - p)\%$. Figure 7 shows the newly constructed time expanded graph for our sample problem instance. With this new TEG, minimizing objective (9) will give us the desired solution. Here, the model solver will decide which $(100 - p)\%$ of the evacuees are the outliers and then direct them through the ‘bypass’ node. As the timestep of this bypass node is zero, the cost for the outlier evacuees will not be added to the final objective. However, as they still have to reach the safe nodes through the road network, they will contribute to the congestion on the road.

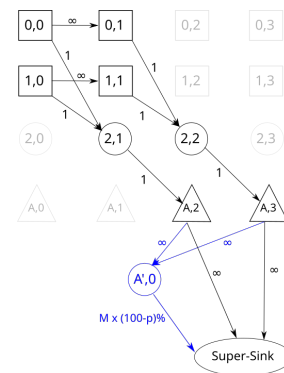


Fig. 7: Extension of the time expanded graph for minimizing Average/Total Evacuation Time of $p\%$ of the evacuees. The blue node denotes the ‘bypass’ node. Edges are labeled with their capacity. M denotes the total number of evacuees.

APPENDIX B
ALGORITHMS

We use Algorithm 3 to calculate the initial feasible solution for our heuristic search method.

Algorithm 3: Calculate Initial Convergent Route Set

Input: Road Network Graph: $\mathcal{G}(\mathcal{N}, \mathcal{A})$

Output: A Convergent Route set

- 1 $\mathcal{A}' \leftarrow \{e(v, u) | e(u, v) \in \mathcal{A}\}$
 - 2 Construct the graph $\mathcal{G}'(\mathcal{N}, \mathcal{A}')$.
 - 3 Add a node v_{sink} to \mathcal{G}' .
 - 4 Add edges $e(v_{sink}, v)$ to \mathcal{G}' , $\forall v \in \mathcal{S}$ with $T_e = 0$.
 - 5 Calculate shortest paths in \mathcal{G}' from v_{sink} to all nodes $v \in \mathcal{N}$ using a single source shortest path algorithm.
 - 6 $routeset \leftarrow$ Shortest paths from v_{sink} to all nodes $v \in \mathcal{E}$.
 - 7 Reverse the direction of each path in $routeset$ and remove node v_{sink} .
 - 8 **return** $routeset$
-

APPENDIX C
CT-DCFP AND O-DCFP SOLUTIONS

In this section, we provide experiment results on the CT-DCFP and O-DCFP problems.

We ran ten experiment runs (with different random seeds) of MIP-LNS for both CT-DCFP and O-DCFP. We again used the one hour time limit for these experiment runs. Figures 8a, 8b, 8c shows a comparison of the A-DCFP, CT-DCFP, and O-DCFP solutions in terms of the three metrics: average evacuation time, evacuation completion time, and non-outlier average evacuation time. Note that, these metrics are also the objectives of A-DCFP, CT-DCFP, and O-DCFP respectively.

From the box-plots we observe that, in general, A-DCFP, CT-DCFP, and O-DCFP solutions are superior compared to the other solutions in terms of the objective they are designed to optimize, respectively. For instance, A-DCFP solutions are, in general, superior than CT-DCFP and O-DCFP solutions in terms of average evacuation time, but worse in terms of the other two objectives. This shows the effectiveness of MIP-LNS and of our formulation in solving evacuation planning problems, while optimizing for different objectives.

APPENDIX D
CALCULATING FLOW CAPACITY OF EDGES

Traffic flow, vehicle speed and traffic density are related by the following equation (Mannering and Washburn [31, Chapter 5, Equation 5.14]):

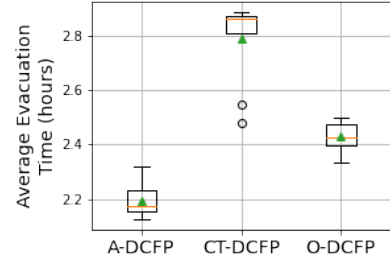
$$q = uk \quad (14)$$

where:

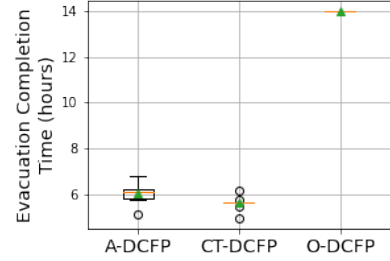
q = Traffic flow (vehicles per time unit)

u = vehicle speed (km per time unit)

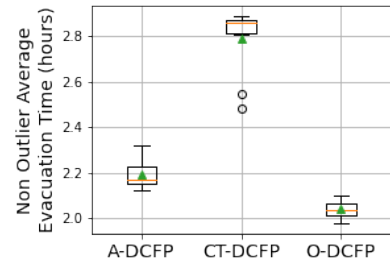
k = Traffic density (vehicles per km)



(a)



(b)



(c)

Fig. 8: Box-plots showing comparison of MIP-LNS solutions for A-DCFP, CT-DCFP and O-DCFP over ten experiment runs. Figures 8a, 8b, 8c show the comparison in terms of the three metrics average evacuation time, evacuation completion time, and non-outlier average evacuation time, respectively. We observe that the A-DCFP, CT-DCFP, and O-DCFP solutions are superior compared to the other solutions in terms of the objective they are designed to optimize, respectively.

For an edge e , let:

l_e = length of edge e (km)

n_e = Number of lanes in edge e

\hat{k}_e = Number of vehicles per lane per km on edge e

Then, we have:

$$k_e = \hat{k}_e n_e \quad (15)$$

We assume that the maximum value of \hat{k} for all edges is:

$$\hat{k}_{max} = 250 \quad [\text{vehicles per lane per km}] \quad (16)$$

$$\implies k_{max} = 250n_e \quad (17)$$

Given a constant travel time t_e for edge e , speed on the edge will be:

$$u_e = \frac{l_e}{t_e} \quad (18)$$

Then, from Equation 14:

$$q_{max} = u_e k_{max} \quad (19)$$

Given a constant travel time for an edge, we use Equation 18 and 19 to calculate the flow capacity of the edge.

APPENDIX E PROOF OF HARDNESS

We point out that CT-DCFP is equivalent to the Confluent Quickest Flow Problem in [18], which the authors have shown the above inapproximability result. In addition, they have also provided a bicriteria hardness result where it is not possible to approximate the completion time within some constant factor even when satisfying only some constant fraction of the demand. For O-DCFP, note that it is a generalization of Problem A-DCFP where $p = 1$. Therefore, any hardness result for A-DCFP also holds for O-DCFP. Thus, we focus on the following two theorems:

The approximation hardness proof of A-DCFP is similar to the one in [18]. The main difference is in its analysis since the objective in the two problems differ. For brevity and completeness, we outline the reductions but omit certain proofs and ask the readers to refer to [18] for more details.

The approximation hardness result relies on the NP-hardness of the capacitated version Two Distinct Path Problem.

Problem 5 (Two Distinct Path Problem). Let G be a graph with two sources x_1, x_2 and two sinks y_1, y_2 . Every edge is labelled with either 1 or 2. Determine if there exists two edge-disjoint paths P_1, P_2 such that P_i is a path from x_i to y_i for $i = 1, 2$ and P_2 only uses edges with label 2 (P_1 can use any edge).

The above problem is known to be NP-hard [33]. Other variations of the problem such as uncapacitated, undirected/directed, edge/node-disjoint paths are also known to be hard (see e.g. [34], [35] and [36]).

Proof of Theorem 2. Given an instance \mathcal{I} of the Two Distinct Path Problem, consider constructing the following graph G where we attach safe node t to y_1, y_2 with an edge of capacity 1, 2 respectively. For $i = 1, 2$, we also add a source s_i and attach it to x_i with an edge of capacity i . Every edge with label i also has capacity i . Source s_i has $M * i$ evacuees for some large M and each edge has a travel time of 1. The upperbound completion time is set to be $M^2 n$.

If there exists two disjoint paths in \mathcal{I} , then a valid schedule simply sends i evacuees at every time step, where the last group of people leaves their sources at time M . Since each path has length at most $n = |V(G)|$, the i evacuee that left source s_i at time k is guaranteed to arrive by time $k + n$. Then, the total evacuation time is at most $\sum_{k=1}^M 3(k + n) =$

$3M^2/2 + 3M/2 + 3Mn$, resulting in an average evacuation time of roughly $M/2$.

If \mathcal{I} does not have two disjoint paths, then consider the two paths P_1, P_2 in a solution to A-DCFP in G . If P_1, P_2 intersects before t , since it is a confluent flow, the edge following their node of intersection is a single-edge cut that separates the sources from the sink. If the two paths only intersects at t , since we are in a NO-instance of \mathcal{I} , P_2 must have used an edge of capacity 1. Then, deleting that edge along with $s_1 x_1$ also separates the sources from the sink. Note that in both cases, the cut has capacity at most 2. Then, at every time step, at most 2 evacuees can cross the cut. Thus, for all $3M$ evacuees to cross the cut, it takes at least $3M/2$ time steps. Due to this bottleneck, it follows that the smallest total evacuation time is at least $\sum_{k=1}^{3M/2} 2(k + n) \geq 9M^2/4$, giving an average of at least $3M/4$.

Since the two instances has a gap of $3/2 - \epsilon$ where ϵ depends on the choice of M , our result follows. \square

The proof of Theorem 3 follows a similar structure. We use the same setup as the proof of log-hardness of Quickest Flow Time in [37] (Theorem 7) with an arbitrarily large upperbound on completion time. Refer to [37] for more details. Note that the resulting graph contains N sources, one safe node and a total of $M^2 \log n$ evacuees. We can similarly show that a YES-instance of the Two-Disjoint Path problem leads to an average evacuation time of at most $M^2/2$. Meanwhile, if it is a NO-instance, then by Lemma 23 in [37], there is cut of capacity at most 2, creating a bottleneck. Using similar analysis as before, one can show that the average evacuation time is at least $M^2 \log N/4$. Then, theorem 3 follows immediately.

Proof of Theorem 1. The proofs for all three problems are similar and hence we only focus on A-DCFP here. Given an instance of k NDP where G is a subgraph of a grid and $k = O(n)$, we first swap the location of the sources and sinks such that all sinks lie on the outer boundary. One can easily check that subdividing any edge and adding a leaf to any vertex of degree less than 4 still ensures that G remains a subgraph of a grid. Then, we claim that without loss of generality, we can assume that all sources and sinks are degree-1 vertices. This can be accomplished by first subdivide every edge and shift the sources/sinks to an adjacent newly added vertex. Then, add a single edge to it and shift the source/sink to the new pendant vertex. This ensures that every source and sink is incident to only one edge. For any edge incident to a source s_i or a sink t_i , assign it a capacity of i ; every other edge has a capacity of k . Each source s_i has demand $M * i$ where $M \geq n^3$. This means in total, there are $M * k^2/2$ evacuees.

In a YES-instance, every source follows its designated path. At every timestep, each source s_i sends i people, ensuring a total of $k^2/2$ people leaves the sources every timestep. Since each disjoint path has length at most n , anyone leaving at time t is guaranteed to arrive by time $t + n$. This implies that the last group, leaving at time M also arrives by time $M + n$,

achieving an average arrival time of at most $\frac{1}{M * k^2 / 2} (k^2 / 2) * \sum_{t=1}^M (t + n) \leq M/4 + n$.

In a NO-instance, in a solution to A-DCFP, consider the cut formed by the edges incident to the sinks. We claim that the amount of flow through this cut at any point in time is at most $k^2/2 - 1$. Assume for the sake of contradiction that there exists some point in time where the flow across the cut is at least $k^2/2$. Since the total capacity of the cut is $k^2/2$, then every edge is used at full capacity at that point in time; in particular, every sink is used in the final routing. Since the routes are confluent, every source is matched to a distinct route. Since we are in a NO-instance, there exists i, j such that source s_i is routed to sink t_j and $i < j$. Since source s_i can send at most i flow at any point in time, sink t_j can never receive its full capacity of j , a contradiction.

Then, at any point in time, at most $k^2 - 1$ people can arrive at the destinations. This implies we need at least $T = M * k^2 / (2(k^2 - 1))$ rounds and thus a total evacuation time of at least $(T^2/2)(k^2 - 1)$. This implies an average evacuation time of at least $Mk^2 / (4(k^2 - 1)) = M/4 + M/(4(k^2 - 1))$. By our choice of M , $M/(4(k^2 - 1)) \geq n$, causing a gap between the YES and NO instances, proving our theorem. \square